AIP | Review of Scientific Instruments

Viscosity measurements of viscous liquids using magnetoelastic thick-film sensors

Keith T. Loiselle and Craig A. Grimes

Citation: Review of Scientific Instruments **71**, 1441 (2000); doi: 10.1063/1.1150477
View online: http://dx.doi.org/10.1063/1.1150477
View Table of Contents: http://scitation.aip.org/content/aip/journal/rsi/71/3?ver=pdfcov
Published by the AIP Publishing

Viscosity measurements of viscous liquids using magnetoelastic thick-film sensors

Keith T. Loiselle and Craig A. Grimes[a)]
Center for Applied Sensor Technology, Department of Electrical Engineering, The University of Kentucky, Lexington, Kentucky 40506

(Received 11 October 1999; accepted for publication 29 November 1999)

A ribbon-like magnetoelastic thick-film sensor can be considered the magnetic analog of an acoustic bell. In response to an externally applied magnetic field impulse the magnetoelastic sensor magnetically rings, in a bell-like fashion, emitting magnetic flux with a characteristic resonant frequency that is determined from a fast Fourier transform of the transient response captured using a pickup coil. The resonant frequency of the sensor changes in response to mass loading and, when immersed in liquid, interfacial shear forces associated with viscosity. We report on the use of magnetoelastic sensors to measure the viscosity and density of highly viscous liquids. When characterizing highly viscous liquids, to avoid over damping of the sensor due to the liquid mass load the sensor is suspended from a boat-like structure with one end of the sensor immersed a fixed distance into the liquid. Using this method liquid viscosities ranging from 1.3 to 12 P are measured.
 [S0034-6748(00)01603-8]

I. INTRODUCTION

Magnetoelastic sensors can be considered the magnetic equivalent of acoustic bells. A magnetic field impulse is used to impart elastic energy into the sensor, which in turn acts to mechanically deform the material in a transitory, time decaying response. Since the sensor material is magnetostrictive, the mechanical deformations result in the emission of a time varying magnetic field from the sensor, detectable from a remotely located pickup coil. Figure 1 is a schematic drawing illustrating the remote query nature of magnetoelastic sensors. Although all frequencies are contained within the magnetic field impulse, elastic waves at frequencies other than the mechanical resonant frequency of the sensor are quickly dissipated. Hence the magnetoelastic sensor magnetically ''rings'' at its resonant frequency. A fast Fourier transform (FFT) of the emitted flux, captured using an oscilloscope connected to a pickup coil[1] enables the resonant frequency of the magnetoelastic sensor to be determined.

Our interest is in the development of inexpensive, remote query sensors for environmental monitoring.[2,3] An advantage of using magnetoelastic sensors is that they are monitored remotely,[4–7] without the need for direct physical connections such as wires or cables, nor line-of-sight alignment as needed with optical detection methods. The magnetic flux can be detected external to the test area, using a pickup coil to enable remote query, *in situ* measurements. Earlier work[7] has shown the use of magnetoelastic sensors for environmental monitoring, with the resonant frequency of the sensor changing in response to pressure, temperature, mass load, and the viscosity of inviscid liquids, such as water. In earlier work the sensor was submerged within the liquid being characterized. However, when immersed within highly viscous liquids, such as engine oil, the liquid medium acted as an effective mass load damping the oscillations of the sensor such that it was no longer detectable. To overcome this limitation two methods have been developed for suspending the sensor such that only a fraction of the sensor is immersed, uniformly, within the fluid. For characterization of constant density liquids, a small boat-like fixture is used that enables the sensor to float upon the surface of the liquid with only the tip of the sensor immersed. The technique allows rapid, *in situ* measurement of highly viscous liquids. We have successfully measured the viscosity of SAE 70 grade motor oil, having a viscosity of 12 P. As the boat can rise and fall with changing fluid levels without affecting the measurement, the method could, for example, be used for *in situ* measurement of engine oil viscosity to help determine when the oil should be replaced. This would avoid waste by discarding the engine oil too early, and engine damage by replacing the oil too late.

Several different viscosity sensors are commercially available for measuring liquid viscosity. For example, one viscometer consists of cylinders enclosed within a fluid-filled chamber, with the viscosity determined from the amount of power needed to rotate the cylinder at constant speed.[8] Another viscometer is based upon a rod, under constant force, traveling inside a fluid-filled tube with the viscosity determined from the time of travel.[9] Piezoelectric transducer ceramics,[10] ultrasonic plate waves,[11] and quartz resonators[12,13] have also been used for viscosity measurements. These methods all require direct electrical connections to the sensor. This is in contrast to the magnetoelastic sensor, where the sensor and detection circuitry have no direct physical connections enabling the detection system to be completely isolated from the liquid environment.

In the original work[7] using magnetoelastic sensors to measure viscosity, the frequency spectrum of the sensor was obtained by sweeping the frequency of the query field and

[a)]Electronic mail: grimes@engr.uky.edu

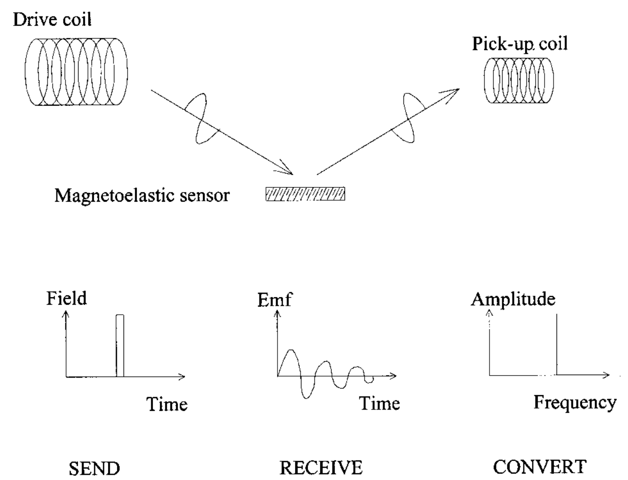

FIG. 1. Schematic drawing illustrating the remote query nature of magnetoelastic sensors.

monitoring the response of the sensor. While this method is highly accurate, with a 0.25 Hz resolution being practical, the measurement requires several minutes. The new magnetoelastic-sensor query method uses a magnetic field impulse to excite the sensor. The transient response of the sensor is captured using an oscilloscope connected to the pickup coil; an illustrative measurement of this response is shown in Fig. 2. The FFT[14] of the transient, time domain response is performed to determine the frequency spectrum of the sensor. A peak in the frequency spectrum indicates the resonant frequency of the sensor; Fig. 3 is the FFT of the data in Fig. 2. The time domain measurements enable the sensor to be characterized in approximately 0.5 s (16 ms for data capture, the balance for data processing), enabling the characterization of quickly changing environments.

II. THEORETICAL MODEL

A theoretical model that describes the frequency response of the sensor to liquid viscosity and density can be derived from the equations of motion for a vibrating thin elastic plate,[15] shown schematically in Fig. 4. With the length of the sensor (plate) oriented along the y axis, and

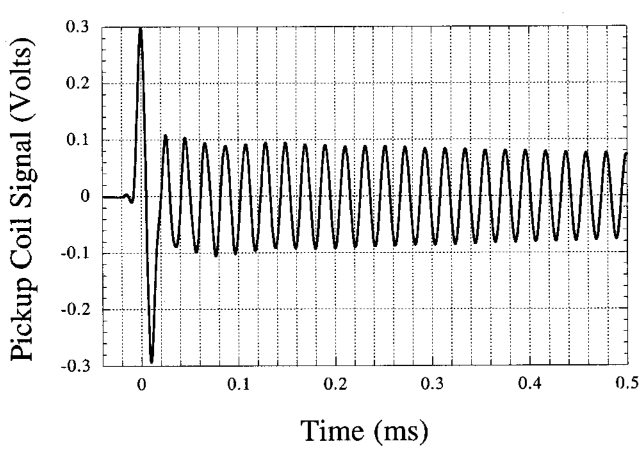

FIG. 2. Typical time-domain response of sensor to magnetic field impulse captured using oscilloscope.

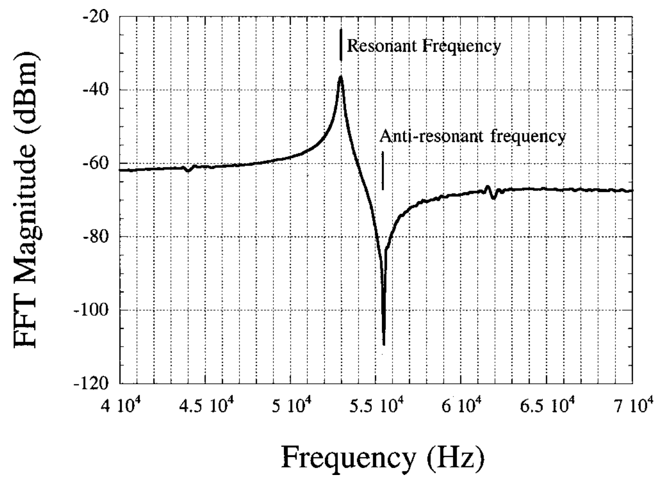

FIG. 3. Output of FFT conversion of time domain response seen in Fig. 2.

width of the sensor along the z axis, in response to a y-directed time varying magnetic field the equation of motion for a sensor in air is[7,15]

$$\rho_s \frac{\partial^2 u_y}{\partial t^2} = \frac{E}{1-\sigma^2} \frac{\partial^2 u_y}{\partial y^2}, \tag{1}$$

where ρ_s is the density of the sensor material, E is Young's modulus of elasticity, σ is the Poisson ratio, and u is the displacement vector of the sensor. While the sensor will exhibit vibrations at almost any frequency, if the frequency of the ac field is equal to the mechanical resonance frequency of the magnetoelastic sensor the conversion of the magnetic energy into elastic energy is maximal and the sensor undergoes a magnetoelastic resonance. Hence we seek a standing wave solution to Eq. (1) in the form

$$u = e^{-i\omega_n t} \cos \frac{n\pi y}{L}, \tag{2}$$

where ω_n denotes the set of the longitudinal resonant radian frequencies of the sensor including higher order harmonics, n denotes integers, t denotes time, and L is the length of the sensor. Our concern is with the fundamental resonant fre-

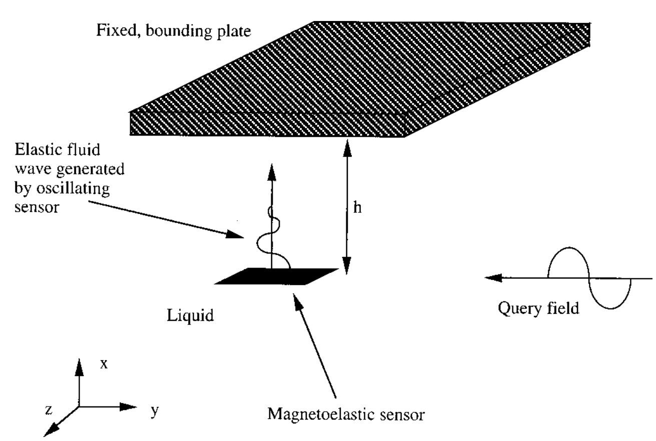

FIG. 4. Sensor geometry used to establish theoretical model of sensor frequency shift due to liquid density and viscosity.

quency, $n=1$, due to its relatively larger amplitude. Solving Eq. (1) after substitution of Eq. (2) we have for the first harmonic frequency[15]

$$f=\sqrt{\frac{E}{\rho_s(1-\sigma^2)}}\frac{\pi}{L}. \tag{3}$$

As can be seen from Eq. (3), the characteristic resonant frequency is dependent on the length, density, Young's modulus, and the Poisson ratio of the sensor.

The resonant frequency of the sensor is also dependent upon details of the interfacial mechanics between the ambient medium and the sensor surface. Upon immersion in a liquid, the resonant frequency of the sensor will be shifted lower due to the dissipative character of the shear forces associated with viscosity. To obtain an expression that correctly relates liquid viscosity to the resonant frequency of the sensor, as shown in Fig. 4 we consider the motion of an incompressible fluid bounded by the oscillating sensor and a parallel-oriented fixed surface distance h from the sensor in the x direction. The sensor vibrates at velocity s, generating an x-directed elastic wave that propagates into the fluid towards the steady plate. The fluid velocity v must satisfy the boundary conditions $v_y=s$ at $x=0$ (v_x and v_z are zero), and $v_y=0$ at $x=h$. From the Navier–Stokes equation the following expression is found for the fluid velocity as a function of distance from the vibrating sensor:[16]

$$\nu=s\frac{\sin k(h-x)}{\sin kx}, \tag{4}$$

where $k=(1+i)/\delta$, $i=\sqrt{-1}$, and $\delta=\sqrt{2\eta/\rho_l\omega}$ is the velocity amplitude damping constant used to quantify the penetration depth of the wave generated by the oscillating surface. ω is the radian frequency, η is the liquid viscosity, and ρ_l is the density of the liquid.

The equation of motion for the sensor immersed in liquid is obtained by using the hydrodynamic form of Newton's law[16] to describe the frictional force on the surface of the sensor due to the liquid viscosity. Inserting this force expression into Eq. (1) we have

$$\frac{\partial^2 u}{\partial t^2}=\frac{E}{\rho_s}\frac{1}{1-\sigma^2}\frac{\partial^2 u}{\partial y^2}-\frac{2\eta k}{\rho_s d}\frac{\partial u}{\partial t}\cot kh, \tag{5}$$

where d is the thickness of the sensor. The factor of two in the second term on the right-hand side of Eq. (5) is due to the sensor having two faces. The dispersion equation relating the radian resonant frequency of the sensor ω to liquid properties is obtained from the solution of Eq. (5).

$$\omega^2=\frac{E}{\rho_s(1-\sigma^2)}\left(\frac{\pi}{L}\right)^2-\frac{2\eta\omega}{\delta\rho_s d}\frac{\sinh(2h/\delta)-\sin(2h/\delta)}{\cosh(2h/\delta)-\cos(2h/\delta)}$$
$$=(\omega_0+\Delta\omega)^2, \tag{6}$$

where ω_0 is the frequency of the sensor in air, and the shift in frequency due to the effects of liquid is downward, $\Delta\omega=\omega_n-\omega_0<0$. The first term on the right-hand side of Eq. (6) represents the response of the sensor vibrating without

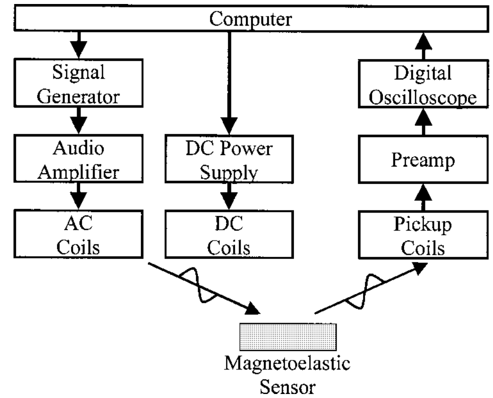

FIG. 5. Block diagram of magnetoelastic sensor query and detection electronics.

damping forces, the second term on the right-hand side reflects the influence of the shear forces acting on both faces of the sensor.

For highly viscous fluids, $(2h/\delta\ll 1)$, Eq. (6) reduces to

$$\Delta f=-\frac{1}{3}f_0\frac{\rho_l h}{\rho_s d}. \tag{7}$$

As the attenuation depth δ is large compared with h, the liquid layer oscillates synchronously with the sensor as if a solidified liquid layer of mass $\rho_l h$ per unit area was loaded on the sensor. In this limit fluid density ρ_l can be measured, but not viscosity.

For inviscid fluids $(2h/\delta\gg 1)$, e.g., water, Eq. (6) reduces to

$$\Delta f=-\frac{\sqrt{\pi f_0}}{2\pi\rho_s d}(\eta\rho_l)^{1/2}. \tag{8}$$

For this regime the frequency shift is proportional to the square root of the liquid viscosity and density product.

III. EXPERIMENTAL RESULTS AND DISCUSSION

Figure 5 is a schematic block diagram of the sensor interrogation electronics. A pair of Helmholtz coils that surround the test area powered by a dc power supply, or a magnetically hard thick film placed adjacent to the sensor, are used to generate a dc magnetic bias field. The dc field is used to partially cancel the magnetic anisotropy of the sensor material, thereby enhancing the magnetoelastic oscillations of the sensor.[17,18] A function generator produces the pulse used to excite vibrations in the sensor, which is then amplified and sent through a single coil or coil pair; the interrogation field does not need to be uniform. The waveform used to excite the sensor in this work consisted of an 8 ms positive 2 Oe pulse, followed by an 8 ms negative 2 Oe pulse; the dc biasing field used was 5 Oe. A 10 cm×10 cm 40-turn pickup coil is used to monitor the sensors, which can be located up to 30 cm away from the pickup coil and still detected. The pickup coil is fed into a low noise preamplifier that includes a 1–100 kHz band pass filter. The output of the preamplifier is sent to a digital oscilloscope. As the resonant frequency of the sensors used in this work were below 60 kHz a 250 kSa/s sampling rate was used, a rate sufficient to satisfy the Ny-

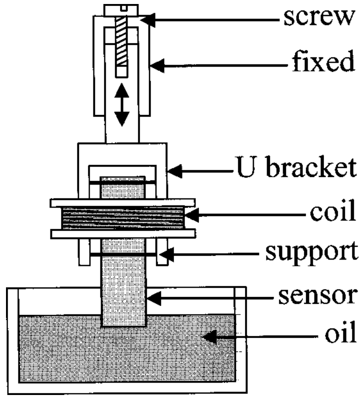

FIG. 6. Schematic drawing of method used for controlled immersion of sensor into liquid.

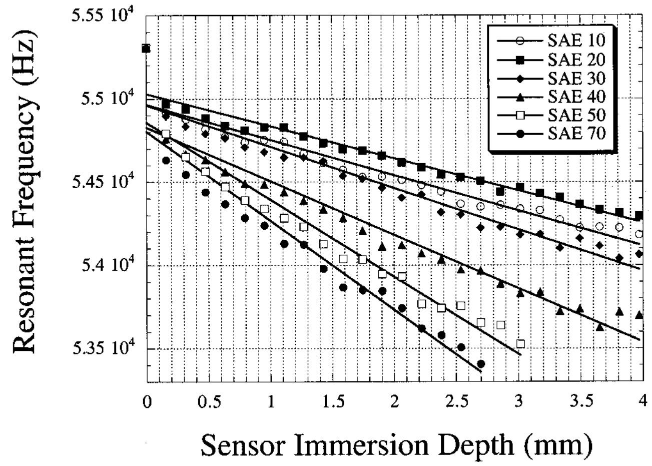

FIG. 7. Resonant frequency of magnetoelastic sensor versus immersion depth, measured for different grade oils.

quist criteria.[19] A 32 768 point FFT is performed on the captured signal. The resolution of the time domain measurement, the sampling frequency divided by the number of samples in the FFT data file, is 7.6. A computer automates the entire process of triggering the pulse and recording the FFT peak from the oscilloscope.

In the earlier work,[7] highly viscous liquids could not be characterized due to the large effective mass load on the immersed sensor, which acted to extinguish the oscillations of the sensor. For a 30 μm thick Metglas[20] 2826 MB alloy sensor, composition $Fe_{40}Ni_{38}Mo_4B_{18}$, a mass load of approximately 20 $\mu g/mm^2$ is sufficient to extinguish the response of the sensor per our electronics. However, by dipping the sensor into the liquid a small fraction of its total length over damping of the sensor is avoided; we find a linear relationship between the distance which the sensor is immersed in the liquid and shift in the sensor resonant frequency.

The first method used for immersing a sensor a controlled distance into the liquid is illustrated in Fig. 6. To avoid over damping the sensor, a $38\times 12.5\times 0.030\,mm^3$ ribbon of Metglas alloy 2826 MB, was woven between waxed strings suspended across a U-shaped bracket, with a screw adjustment used to raise or lower the sensor. This method was used to explore the relationship between the resonant frequency shift of the sensor versus depth in the oil, and to determine the maximum depth that the sensor can be lowered before its vibrations become over damped (nondetectable using our equipment). Starting with the sensor just above the surface of the liquid, the sensor was dipped into the oil by 159 μm increments, corresponding to 1/8th screw turn, from 0 to 4 mm. The sensor was immersed into six different weight motor oils, SAE 10, 20, 30, 40, 50, and 70, with the resonant frequency of the sensor recorded as a function of immersion distance.

As seen in Fig. 7, a highly linear relationship between the depth of sensor immersion and resonant frequency shift are seen. For the two highest viscosity oils, SAE 50 and 70, the sensor became over damped at, respectively, 3.0 and 2.7 mm, immersions. As seen in Fig. 8, for fixed immersion depth the resonant frequency of the sensor linearly tracks the square root of the density and viscosity product (units$=$kg m^{-2} s$^{-1/2}$). Viscosity measurements were calibrated using a standard falling-ball type viscometer, with all measurements taken at 19 °C, measured values ranged from 1.3 Poise for the SAE 10 grade oil, to 12 Poise for SAE 70. The density was essentially constant for the six oils, ranging from 0.89 to 0.92 g/cm^3.

It is worth noting that as the sensor first touched the surface of the oil, surface tension caused the oil to climb upwards on the sensor (wicking) resulting in a large change in the resonant frequency, see Fig. 7. This large change in the resonant frequency upon initial contact between the sensor and liquid was consistent across the different weight oils. The shift in the resonant frequency upon initial contact with the liquid, i.e., the frequency shift due to wicking, might serve as a useful diagnostic tool for characterizing the surface tension of equal density liquids. For example, detergents are often added to motor oil to reduce the surface tension enabling the oil to hold dirt particles in suspension longer. The objective is to suspend the dirt particles long enough for the oil to carry the dirt particles to the filter where they are trapped, instead of depositing them in the engine.

The further the sensor is immersed in the liquid, the greater the surface area exposed to the liquid, and hence the

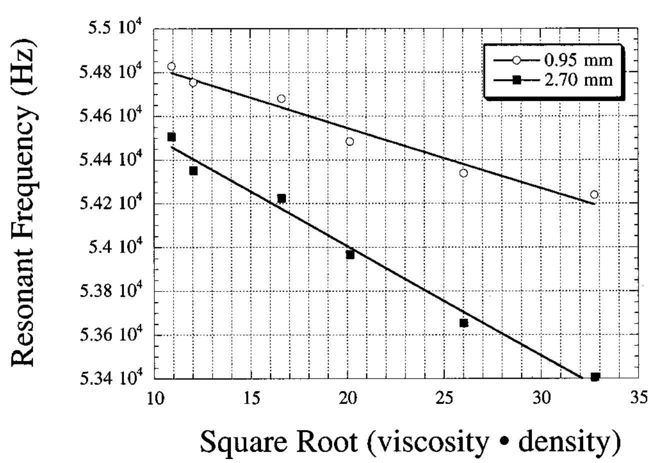

FIG. 8. Resonant frequency of magnetoelastic sensor versus square root of viscosity and liquid density product, units$=$kg m^{-2} s$^{-1/2}$, for sensors held at immersion depths of 0.95 and 2.70 mm.

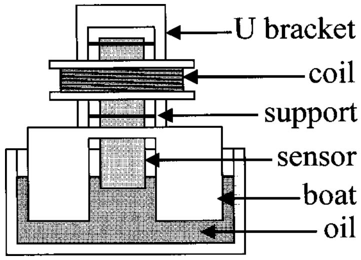

FIG. 9. Schematic drawing of floating-boat apparatus used to hold sensor at a fixed immersion depth.

greater the sensitivity of the sensor to liquid viscosity. The sensitivity of the sensor is dependent upon the distance it is immersed in the liquid. This effect can be seen in Fig. 8, where the sensor immersed 2.70 mm has a steeper slope than the sensor immersed 0.95 mm. For the 2.70 mm immersed sensor, the 7.6 Hz measurement resolution corresponds to a measurement error of 6.2 cP; for the 0.95 mm immersed sensor the measurement resolution is 11.7 cP. Greater resolution can be obtained by increasing the number of data points used in the FFT operation. However, the limit of the Hewlett-Packard 54810A Infiniium oscilloscope used in this work was 32 768 samples.

The second method used for dipping the sensor was designed to achieve a consistent sensor immersion depth, and hence sensitivity, for use in environments where absolute fluid levels were changing. Referring to Fig. 9, the same U-shaped bracket seen in Fig. 6 is mounted onto a circular, doughnut-shaped boat, with the sensor suspended through the open center of the boat into the liquid. As long as the density of the liquid remains constant the sensor will remain immersed at a constant depth in the liquid although the absolute fluid level may change. Figure 10 shows the resonant frequency of the boat-mounted sensor, extending 2.5 mm into the liquid, versus the square root of the viscosity and density product. The sensor is clearly operating in the second regime as described by Eq. (8). Two equal oil mixtures of SAE 40 with 50, and SAE 50 with 70, were used in addition

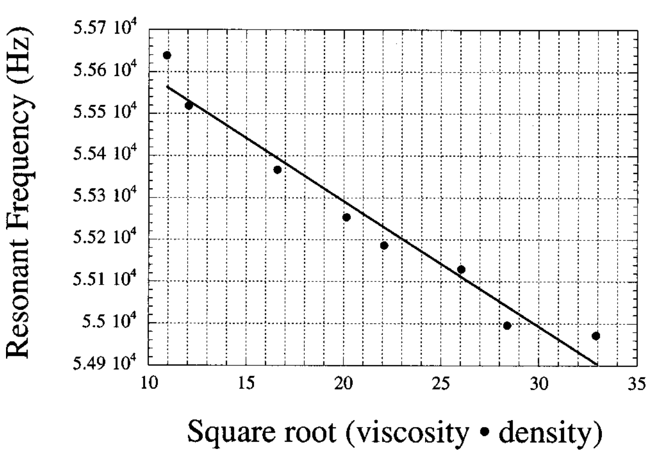

FIG. 10. Resonant frequency of magnetoelastic sensor, immersed 2.5 mm into liquid using boat method, vs square root of the liquid density and viscosity product (units=kg m^{-2} $s^{-1/2}$). The density of SAE 10–70 grade oil is essentially constant, enabling the boat method to accurately track changes in viscosity.

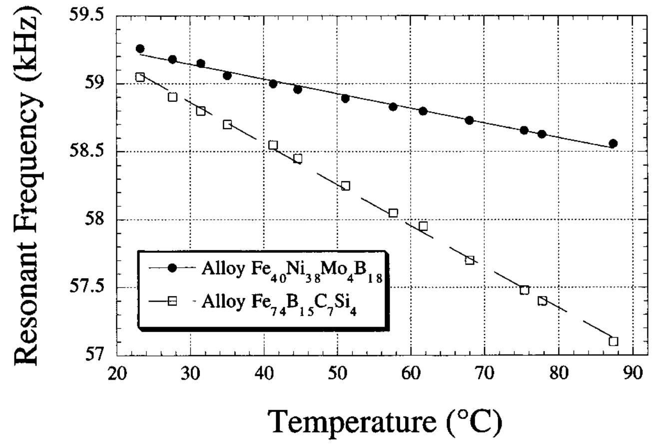

FIG. 11. Resonant frequency of two magnetoelastic sensors, composition $Fe_{40}Ni_{38}Mo_4B_{18}$ and $Fe_{74}B_{15}C_7Si_4$, as a function of temperature. For sensors of equal surface roughness, the absolute frequency difference stays constant whether immersed in liquid or measured in air, enabling simultaneous measurement of viscosity and temperature.

to the pure grades to expand the range of viscosity measurements.

As a related measurement issue, as is well known, viscosity is highly temperature dependent.[13] Consequently, to compare isothermal viscosities of different liquids it is necessary to accurately measure temperature. As seen in Eq. (3), the resonant frequency of the sensor is dependent upon Young's modulus, which is temperature dependent.[21] Figure 11 shows the temperature response of two Metglas sensors, composition $Fe_{40}Ni_{38}Mo_4B_{18}$ and $Fe_{74}B_{15}C_7Si_4$. The difference in resonant frequency between the two sensors of different alloy composition is constant independently of whether they are in air or liquid, so long as the sensors have the same degree of surface roughness. Hence, cross-correlation between the two magnetoelastic sensors enables isothermal calibration of the viscosity measurement.

As described in Ref. 22 a sensor with a large surface roughness traps liquid near its surface, so that it responds only to liquid density as quantified by Eq. (7). Hence viscosity and liquid density effects can be separated through cross-correlating the responses of magnetoelastic sensors with rough and smooth surfaces. As seen in Fig. 11, cross correlation between sensors of different alloy composition but equal amounts of surface roughness would enable instantaneous measurement of temperature and viscosity.

The magnetoelastic thick-film sensors used in this work were purchased from Allied Signal Corporation,[20] alloys 2826MB and 2605SC. Prior to use the ribbons were vacuum annealed at 200 °C for 1 h to remove residual stresses associated with the ribbon fabrication process. After the annealing step, the sensors are stable up to 150 °C, the upper temperature tested. The $38\times12.5\times0.030\ mm^3$ sensors have a unit material cost of approximately $0.005.

ACKNOWLEDGMENTS

Support of this work by the Life Sciences Division of the National Aeronautics and Space Administration of the United States of America under Grant No. NAG5-4594, and by the National Science Foundation under contract Nos. ECS-9701733 and ECS-9875104 is gratefully acknowledged. One of the authors (K. L.) is supported through the NSF funded IGERT *Integrated Sensing Architectures* program.

[1] H. J. Oguey, Rev. Sci. Instrum. **31**, 701 (1960).
[2] P. G. Stoyanov, S. A. Doherty, C. A. Grimes, and W. R. Seitz, IEEE Trans. Magn. **34**, 1315 (1998).
[3] C. A. Grimes, P. G. Stoyanov, Y. Liu, C. Tong, K. G. Ong, K. Loiselle, S. A. Doherty, and W. R. Seitz, J. Phys. D **32**, 1329 (1999).
[4] J. M. Barandiaran and J. Gutierrez, Sens. Actuators A **59**, 38 (1997).
[5] J. Ryan, Jr., Sci. Am. 120 (1997).
[6] E. E. Mitchell, R. DeMoyer, and J. Vranish, IEEE Trans. Ind. Electron. **33**, 166 (1986).
[7] C. A. Grimes, K. G. Ong, K. Loiselle, P. G. Stoyanov, D. Kouzoudis, Y. Liu, C. Tong, and F. Tefiku, J. Smart Mater. Struct. **8**, 639 (1999).
[8] See product information at: http: //www.nametre.com/products.htm
[9] See product information at: http://www.cambridge-applied.com/tech/viscometers.html
[10] See product information at: http://www.vtip.org/Licensing%20Opportunities/vtip%20disclosures/95-033.html
[11] K. K. Kanazawa and J. G. Gordon II, Anal. Chim. Acta **175**, 99 (1985).
[12] B. A. Martin, S. W. Wenzel, and R. W. White, Sens. Actuators A **21–23**, 704 (1990).
[13] Z. A. Shana, D. E. Radtke, U. R. Kelkar, F. Josse, and D. T. Haworth, Anal. Chim. Acta **231**, 317 (1990).
[14] Rodger E. Ziemer, William H. Tranter, and D. Ronald Fannin, *Signals and Systems: Continuous and Discrete*, 3rd ed. (Macmillan, London, 1993), p. 173.
[15] L. D. Landau and E. M. Lifshitz, *Theory of Elasticity*, 3rd ed. (Pergamon, New York, 1986), Chap. II.
[16] L. D. Landau and E. M. Lifshitz, *Fluid Mechanics*, 2nd ed. (Pergamon, New York, 1987), Chap. II.
[17] J. M. Barandiaran, J. Gutierrez, B. Hernando, and A. Garcia-Arribas, Int. J. Appl. Electromagn. Mater. **5**, 75 (1994).
[18] P. M. Anderson III, J. Appl. Phys. **53**, 8101 (1982).
[19] See for example, L. B. Jackson, *Signals, Systems, and Transforms* (Addison-Wesley, Reading, MA, 1991), p. 171.
[20] Metglas™ is a trademark of the Allied Signal Corporation. See product information at: http://www.electronicmaterials.com/products/amorph/index.htm
[21] T. Shinoda, N. Soga, T. Hanada, and S. Tanabe, Thin Solid Films **293**, 144 (1997).
[22] F. Herrmann, D. Hahn, and S. Buttgenbach, Appl. Phys. Lett. **74**, 3410 (1999).